

REFRACTIVE INDEX MATCHED LDA TECHNIQUE FOR INVESTIGATIONS OF LAMINAR TO TURBULENT BOUNDARY LAYER TRANSITION

S. Becker

Institute of Fluid Mechanics (LSTM)
Friedrich-Alexander University Erlangen-Nuremberg, Cauerstr. 4
D-91058 Erlangen-Nuremberg, Germany
sbecker@lstm.uni-erlangen.de

C. Stoots

Institute of Fluid Mechanics (LSTM)
Friedrich-Alexander University Erlangen-Nuremberg, Cauerstr. 4
D-91058 Erlangen-Nuremberg, Germany
cstoots@lstm.uni-erlangen.de

H. Lienhart

Institute of Fluid Mechanics (LSTM)
Friedrich-Alexander University Erlangen-Nuremberg, Cauerstr. 4
D-91058 Erlangen-Nuremberg, Germany
lienhart@lstm.uni-erlangen.de

D. M. McEligot

Thermal Science and Engineering Laboratory
Idaho National Engineering and Environmental Laboratory (INEEL),
P.O. Box 1625, Idaho Falls, ID 83415, MS 3885, USA
dm6@inel.gov

F. Durst

Institute of Fluid Mechanics (LSTM)
Friedrich-Alexander University Erlangen-Nuremberg, Cauerstr. 4
D-91058 Erlangen-Nuremberg, Germany
durst@lstm.uni-erlangen.de

ABSTRACT

Usage of laser-Doppler anemometry (LDA) requires optical access to the flow field of interest. This is not always easy, as in the case of complex geometries or very near-wall boundary layer measurements. One solution is to employ a solid material and fluid of the same index of refraction. In this case, there is no optical interference of the solid with the LDA. Although this technique is not new, previous studies have been limited to small flow apparatuses and relatively unpleasant fluids. Two new large scale flow facilities (LSTM and INEEL) have now been constructed which permit matched index of refraction (MIR) LDA measurements in difficult geometries at higher Reynolds numbers and with increased spatial resolution in the measurements. This paper describes the facilities and fluid, flow quality, and presents some new fundamental measurements for the transition process in flat plate boundary layers downstream of two-dimensional rectangular ribs. By use of LDA and a large MIR flow system, data for wall-normal fluctuations and Reynolds stresses were obtained in

the near wall region to $y^+ < 0.1$ in addition to the usual mean streamwise velocity component and its fluctuation. Consequently, results covered boundary layers which retained their laminar characteristics through those where a turbulent boundary layer was established shortly after reattachment downstream from the forcing rib. For "large" elements, evolution of turbulent statistics of the viscous layer for a turbulent boundary layer ($y^+ < \sim 30$) was rapid even in flows where the mean velocity profile still showed laminar behaviour.

INTRODUCTION

Laminar to turbulent flow transition is a phenomenon which continues to be of interest to fluid mechanics researchers. Although investigations of laminar to turbulent flow transitions have been going on for many decades, there are still many open questions that await answers. Previously, only limited answers could be provided due to a lack of suitable measuring techniques and/or lack of computational capabilities to study in detail transitional flows. It is only in the

last decade that computing techniques have reached a maturity that permits refined numerical studies of the complex flow structures at the initial stages of transition. The numerical methods now permit study of the flow region where strong non-linear flow interactions occur before the flow enters the state of being fully turbulent. LDA has also finally reached a state of development to permit non-intrusive measurements with sufficient time and spatial resolution to study transitional flows. When complemented by numerical methods, LDA provides a powerful tool to study laminar to turbulent flow transition.

Quantification of boundary layer transitional flows requires measurements very close to the wall for determination of the wall shear stress. However, the very high velocity gradients near the wall raise questions regarding data accuracy for both numerical and experimental investigations. The difficulties in making measurements very near the wall have resulted in few prior experimental studies in the region of $y^+ < 2.5$, and none for $y^+ < 0.25$. Hot wires for near-wall velocity studies are intrusive and pose wall heat conduction problems. LDA measurements usually suffer from optical interference of the laser beams, especially when systems for two and three component measurements are employed. Some examples of near wall flow experimental studies in fully developed pipe flows include Lekakis et al. (1994), and Durst et al. (1995). Similar measurements in fully developed channel flows were conducted by Djenidi and Antonia (1993)

One way to eliminate optical interference of multi-component LDA systems is by employing suitable transparent wall materials together with fluids that possess the same refractive index as the wall material itself. In this way, the wall disappears optically (and therefore has no influence on the laser beams) but maintains its full mechanical influence on the flow. However, no refractive index matched flow facility has existed that permitted flat plate boundary layers to be set up and, hence, provide the basic test facility to study in detail laminar to turbulent boundary layer transition.

It is the aim of this work to study the boundary layer transition process on a flat plate for different cases: behind rectangular rib roughness elements and behind suction arrays. Schlichting (1979) noted behind circular roughness elements two major transition cases:

- disturbances created are initially damped in the flow behind the roughness element and develop slowly
- transition initiates directly behind the roughness element.

FLOW FACILITY AND INSTRUMENTATION

The facility size can also help in making very near-wall velocity measurements by increasing flow

length scales relative to measurement probe size. Until recently, however, no refractive index matched flow facility existed that permitted reasonably-sized flat plate boundary layers to be set up and, hence, provide the basic test facility to study in detail techniques for laminar to turbulent boundary layer transition control.

Design of the Flow Facilities

Of these two flow facilities, the LSTM MIR is the newest. This facility is sketched in Figure 1. Flow is counterclockwise in the figure. The main flow pump is in the lower left corner. From the main pump the working fluid, a light mineral oil, passes through an expansion bellow, diffuser, two elbows, and enters the settling chamber. The settling chamber has several screens and a honey comb for flow conditioning. After the settling chamber, the oil passes through a contraction, enters the test section, and ultimately returns to the main pump.

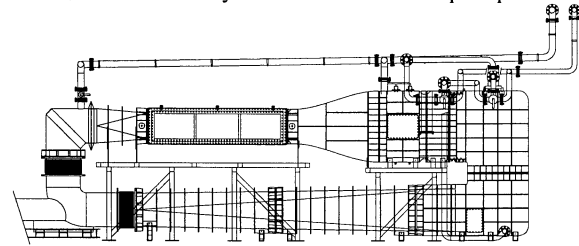


Figure 1 : Schematic sketch of the LSTM MIR facility

	INEEL	LSTM
Test section size	0.62 x 0.62m	0.6 x 0.45m
Test section length	2.4m	2.52m
Contraction ratio	4:1	6:1
Oil	Drakeoil 5 (PENRECO)	Odina 913 (SHELL)
Refractive index	1.4585	1.4585
Kinematical viscosity	14e-6 m ² /s	12e-6 m ² /s
Temperature control	External	Internal
Maximum velocity	1.9m/s	5m/s
Turbulence intensity	0.5%	0.1%

Table 1 : Specifications of the different Matched Index Refraction Tunnels.

The MIR facility at the INEEL is of a similar design. One difference between the two facilities is their maximum Reynold's numbers. The maximum fluid velocity for the LSTM MIR is a factor of 2.5 higher than that for the INEEL facility. An advantage of the INEEL MIR facility is its slightly

larger test section. All important specifications are summarized in Table 1.

Since index of refraction is temperature dependent, temperature control of the fluid is very important. The LSTM facility uses heat input from the main flow pump for heating and has a water-to-oil heat exchanger within the settling chamber for cooling. The water flow rate through the heat exchanger is feedback controlled based upon the oil temperature exiting the test section. The INEEL facility extracts a percentage of the flowing oil, sub-cools it with a oil-to-water heat exchanger, heats it with a computer-controlled electrical heater, and re-injects the oil downstream from the pump.

Flow Qualities

Vertical profiles of velocity were measured at the test section entrance for three fluid velocities. At the entrance, the uniformity in velocity was about 0.2% for the LSTM channel (Figure 2) and about 1% of the mean velocity for the INEEL test facility.

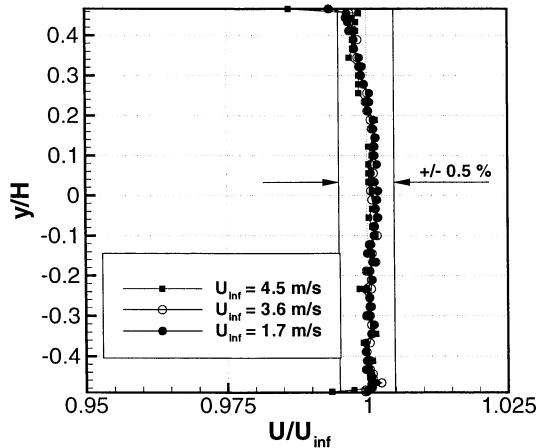


Figure 2 : Vertical velocity profiles across test section 0.27 m downstream of test section entrance

Concerning the INEEL MIR, it is thought that the higher velocity in the upper half of the test section is due to some detachment occurring in the lower part of the elbow entering the settling chamber. At 1.2 m downstream, the non-uniformity in the velocity profile was less than 0.1% of the mean.

Facility Instrumentation

Facility instrumentation can be divided into control / monitoring instrumentation and experimental measurement instrumentation. Velocity and turbulence measurements are obtained primarily with a two-component, fiber optic-based LDA operated in forward or back scatter mode. When operated in the forward scatter mode, custom-built receiving optics from the LSTM are used.

Although the back scatter LDA mode is more convenient for operation, the forward scatter signal-to-noise ratio is 10 to 100 times higher, resulting in

superior signal quality and validation rates, especially near an obstacle or wall. This is illustrated in Figure 3, which compares velocity data obtained in forward scatter versus back scatter. In these measurements, the LDA measurement volume was first positioned in the free stream and the data rates for forward and back scatter were made the same by adjusting the photomultiplier voltage.

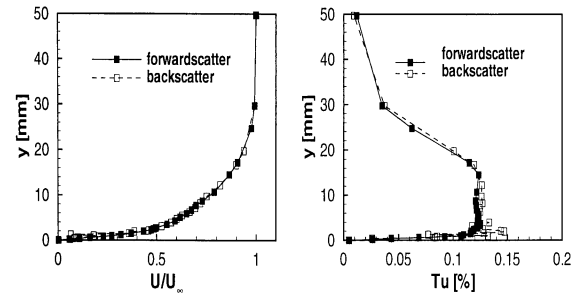


Figure 3 : Comparison of measurements made in forward scatter versus back scatter

Then, the measurement volume was traversed within the boundary layer. Within the boundary layer, the forward scatter configuration exhibited a greater data rate, higher signal to noise ratio, and superior burst quality, resulting in improved burst processing accuracy. Thus, both test sections were designed specifically for optical access on all sides such that LDA measurements in forward scatter can be performed. The LDV measurement control volume diameters are approximately 60 μm . Traversing systems are integrated with the LDVs to allow movement in all three axes.

EXPERIMENTAL RESULTS

Previous experimental investigations of roughness-induced boundary layer transition have been limited to two dimensional circular wire roughness elements (Klebanoff and Tidstrom, 1972). These measurements were performed using one-dimensional hot-wire techniques. In addition to mean velocity and turbulence intensity distributions in the free stream direction, the spectral density distributions were reported for a range of Reynolds numbers. They concentrated on disturbance growth in a "laminar recovery" before transition. Their investigation showed that it is possible to understand the behaviour of the boundary layer in their flows by considering wave disturbances. Stability theory supported these conclusions. Little information exists about the behaviour of the transition process and the flow structure very close to the wall, especially for other velocity components.

Schlichting (1979) shows that the influence of a roughness element upon the transition process can extend between two limits. He suggests that in the case where the disturbance by the roughness element is less than the freestream turbulence intensities, the

effect upon transition is negligible. Then the transition process is located at the same streamwise location as would be predicted for natural transition. The other extreme is when the transition process begins directly behind the roughness element. Data for two-dimensional circular roughness elements indicate that these limits are approximately given by $k^+ < 7$ and $k^+ > 20$, respectively. The present authors' interests center upon the transition process between these two cases. Detailed velocity and turbulence measurements were obtained for a range of laminar and transitional flows.

The measurements with a rectangular rib were carried out at three different roughness heights k and three different freestream velocities, resulting in the following ranges of experimental parameters:

- $k^+ = 5.5$ to 21 , $0.3 < k/\delta_1 < 1$,
- $180 < Re_k < 740$, $6 \times 10^4 < Re_{x,k} < 1.5 \times 10^5$,
- $Re_\theta < 660$, $-125 < (x-x_k)/k < 580$.

For comparison to accepted analytical results, measurements were also conducted without a rib in the model, i.e., a smooth flat plate. Figure 4 shows schematically the test apparatus.

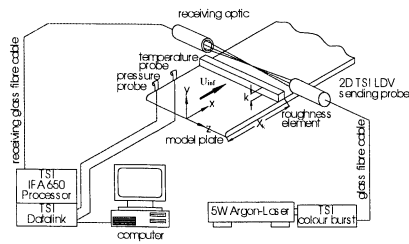


Figure 4 : Schematic of measurement system and flat plate / rib apparatus.

Smooth plate

Initial experiments were conducted with a smooth plate model to qualify the facility as providing data in agreement with existing theory and to serve as a reference condition ($k = 0$) for the effects of rectangular roughness elements. Figure 5 summarises some of the results. The subfigure examines the variation of freestream velocity in the streamwise direction along the length of the plate. Values from the location where the rib would be placed and further downstream varied less than one per cent, indicating a near constant freestream velocity distribution along the plate and a negligible streamwise pressure gradient. Following a procedure which used the displacement thickness of the boundary layer at each streamwise measurement position, a virtual plate origin (x_v) of -209 mm was calculated. In this way, the streamwise mean velocity distribution can be compared to predictions from the boundary layer theory of Blasius (Schlichting, 1979). Figure 5 demonstrates excellent agreement.

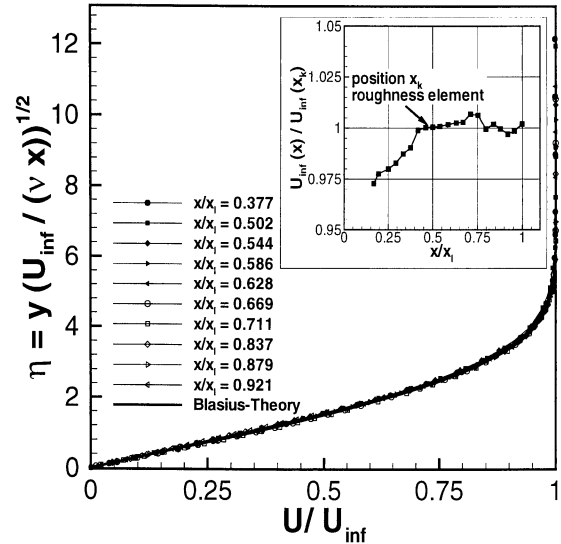


Figure 5: Velocity distribution in the flat plate boundary layer without a roughness element.

Structure of the transition process

The typical evolution of the flow and the effects of the roughness element on the streamwise velocity component are demonstrated in Figures 6a-c. These measurements were obtained with the largest roughness element, $k = 6$ mm, and nominal free-stream velocities of 0.75 , 1.25 and 1.75 m/sec. Results are normalized with the roughness height and the freestream velocity.

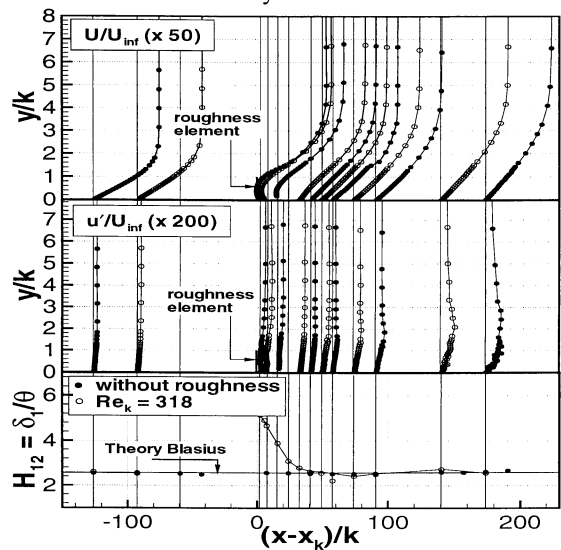


Figure. 6a: Evolution of flow over a two-dimensional rectangular rib. $Re_{x,k} = 6 \times 10^4$, $k^+ = 11$, $k/\delta_1 = 0.7$, $Re_k = 318$

The first case shown ($k^+ = 11$, Figure 6a) appears to correspond to the study of Klebanoff and Tidstrom (1972) with recovery to a laminar mean velocity profile following reattachment at 16 to 25 heights downstream. In the recirculating region and in the boundary layer above it u' is low, approaching the freestream value gradually as y increases.

Downstream the shape factors agree with the Blasius theory but the u' distributions show evidence of growth of disturbances evolving from the level of the inflectional region of the separated profiles ($y/k = 1.5$ or so). At $(x-x_k)/k = 140$ or $x = 2000$ mm, the maximum value of u' in the boundary layer is about twice the freestream value; the quantity u'/u'_{inf} is about 2.5 times its value at the same location on the smooth plate.

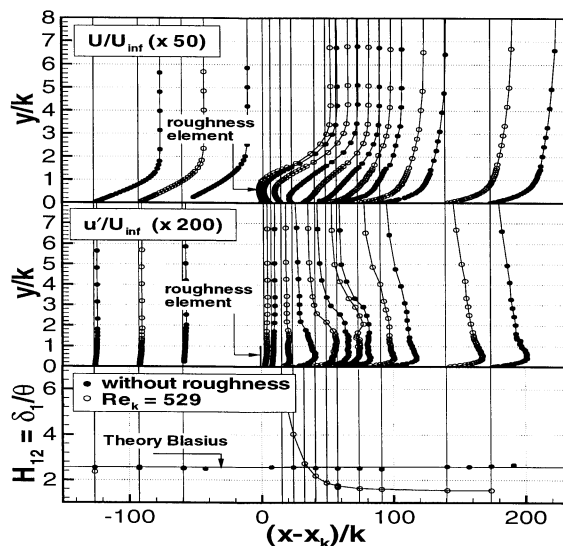


Figure 6b: Evolution of flow over a two-dimensional rectangular rib. $Re_{x,k} = 1 \times 10^5$, $k^+ = 16$, $k/\delta_1 = 0.9$, $Re_k = 529$

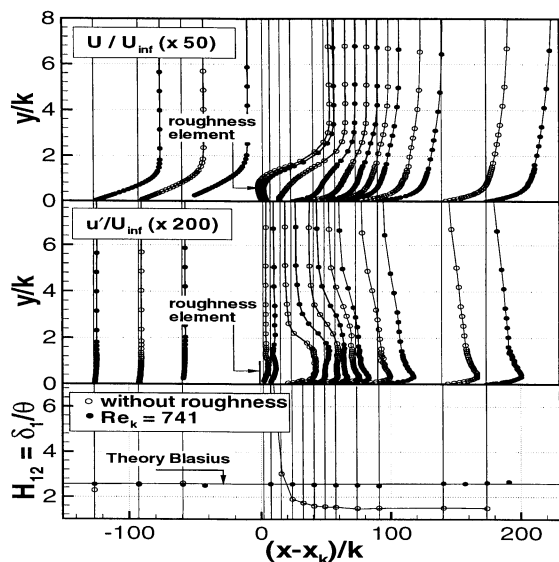


Figure 6c: Evolution of flow over a two-dimensional rectangular rib. $Re_{x,k} = 1.4 \times 10^5$, $k^+ = 21$, $k/\delta_1 = 1$, $Re_k = 741$.

In the second and third cases ($k^+ = 16$, Figures 6b-c) the profiles and shape factors indicate a more obvious transition towards a turbulent boundary layer. After reattachment, the shape factors decrease to values of about 1.5 to 1.6, characteristic of fully-

developed turbulent boundary layers. For the range $75 < (x - x_k)/k < 175$ the deduced local skin friction coefficients agreed with a correlation for a fully-developed turbulent boundary layer.

Klebanoff and Tidstrom (1972) suggested that for much "larger" roughness elements than in their investigation, the inflectional nature of the velocity profile may be such that the instability will be characteristic of a free shear layer rather than the boundary-layer type they studied. The third case likely represents such a situation. In the last profile before reattachment, over a range from near the wall to $y/k = 1.6$ (which corresponds to the inflectional point in the mean velocity profile at that location) u' is approximately six times its freestream value. Reattachment appears to be closer to the rib than for the first and second cases, despite the higher Reynolds number. At $(x-x_k)/k = 25$, the first measurement location after reattachment, normalization by wall variables shows the near-wall region already to be approaching the behavior of the viscous layer of a fully-developed turbulent flow.

Detailed results are presented to examine the evolution of turbulent momentum transport, as represented by the Reynolds shear stress, for different situations. One example should demonstrate the development of a turbulent boundary layer. Nominal values of roughness parameters were $k^+ = 14$, $k/\delta_1 = 0.7$, $Re_k = 502$ and $Re_{x,k} = 1.5 \times 10^5$. Mean streamwise velocity profiles again show mean reattachment between 24 and 38 heights downstream.

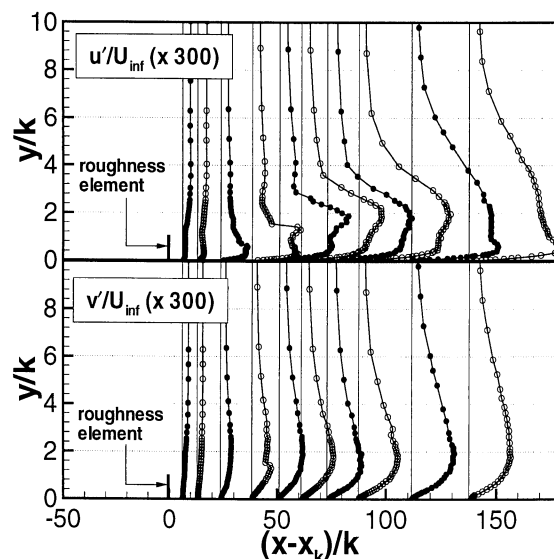


Figure 7a: Evolution of turbulent boundary layer. Results normalized by freestream velocity and rib height

The Reynolds stresses mostly grow as the flow progresses downstream, as expected. The last measurement location before reattachment displays a substantial increase in u' and a moderate increase in v' (Figure 7a). The peak value of u' is about four

times the freestream value. This peak is approximately at the dividing mean streamline and decreases as y increases towards the inflection point in the mean velocity profile

After reattachment the first mean velocity profile, $(x-x_k)/k = 40$, appears to the eye almost like a Blasius profile and the shape factor is near the value for laminar flow with a negligible streamwise pressure gradient. However, the turbulent fluctuations have grown substantially. Two peaks appear in the u' profile, one near the wall and the other at $y/k = 1.4$, near the upstream inflectional region. Both are approximately six times the freestream value and both grow as the flow proceeds downstream. The outer grows more rapidly at first but eventually the highest values occur near the wall at $y/k = 1/2$ as the shape factor decreases to 1.6 and the mean velocity profile becomes more representative of a turbulent boundary layer. From $(x-x_k)/k = 50$ on, the v' distribution has smooth profiles with gentle maxima varying in position from $y/k = 2$ to 1.4 to 1.9-2.0 again, corresponding to the upstream inflectional region.

Further insight is obtained by presenting the data of Figure 7a in terms of wall coordinates, as done in Figure 7b. Only the locations following reattachment are shown since the wall shear stress is in the opposite direction in the recirculating region. At $(x-x_k)/k = 50$, the mean velocity profile still appears to correspond to a Blasius profile in semi-logarithmic coordinates with $\delta^+ = 80$. However, u^+ diverges from $y^+ = 5$, as for the viscous layer of a turbulent boundary layer, and values are below the old "buffer layer" approximation until $y^+ = 20$. This observation is an indication of significant momentum transport by other than molecular means in this range. The two peaks in $(u')^+$ are about 2.2 at $y^+ = 10$ and 2.9 at $y^+ = 35$. The maximum for $(v')^+$ is about unity at $y^+ = 40$. For fully-developed, high-Reynolds-number pipe flow, the values would be $(u')^+ = 2.6$ at $y^+ = 15$ and $(v')^+$ about unity at $y^+ = 100$ (Durst et al., 1995). The Reynolds shear stress demonstrates significant turbulent momentum transport in a thin layer, say $10 < y^+ < 40$. It increases smoothly to a maximum value $(u'v')^+ = 0.9$ at $y^+ = 25$ and then decreases to the edge of the boundary layer.

As the flow progresses downstream, the mean velocity profiles evolve to the logarithmic-"law" shape characteristic of a turbulent boundary layer, and δ^+ increases to about 200 at the last profile. In terms of wall coordinates, the $(v')^+$ maximum retains its value near unity and gradually shifts to higher y^+ without a change in profile shape. This trend corresponds to the peaks at larger y/k and to an increase in τ_w with x . The outer peak in $(u')^+$ retains its magnitude until $(x-x_k)/k = 90$ and then decreases and loses its identity. The inner peak grows slightly and becomes established at $(u')^+ \approx 2.5$ at $y^+ \approx 15$.

The layer of turbulent momentum transport broadens as the flow proceeds downstream. But beyond $(x-x_k)/k = 60$ it does not "penetrate" closer to the wall. The profile becomes approximately self-preserving in wall variables from the wall to $y^+ = 20$. The Reynolds shear stress distribution shows the maximum turbulent momentum transport located in a range about $20 < y^+ < 40$ until $(x-x_k)/k = 90$ with $(u'v')^+$ values near unity, corresponding to a constant stress layer. Then at later stations it "spreads" and decreases in magnitude. As a first approximation, one may say that the important viscous layer becomes established rapidly while the turbulent transport is developing and spreading in the outer region.

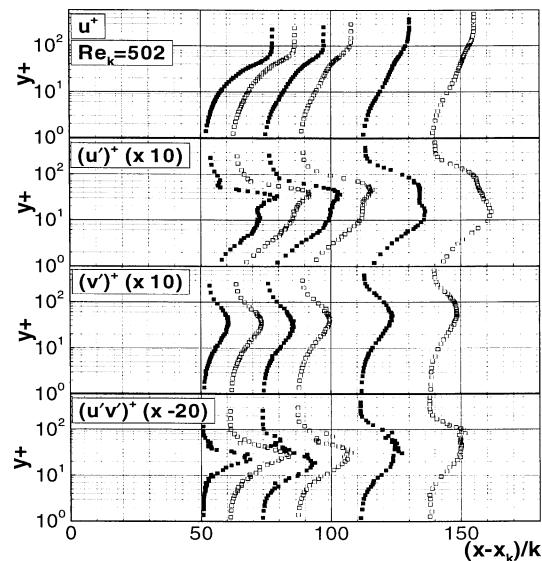


Figure 7b: Evolution of turbulent boundary layer. Wall coordinates.

References

- Djenidi, L., Antonia, R. A., 1993, "LDA measurements in low Reynolds number turbulent boundary layer," *Experiments in Fluids*, Vol 14, pp. 280-288.
- Durst, F., Jovanovic, J., and Sender, J., 1995, "LDA measurements in the near wall region of a turbulent pipe flow," *Journal of Fluid Mechanics*, Vol. 295, pp. 303-335.
- Klebanoff, P. S., and Tidstrom, K. D., 1972, "Mechanism by Which a Two-Dimensional Roughness Element Induces Boundary-Layer Transition", *Phys. Fluids*, 15, pp. 1173-1188.
- Lekakis, I., Durst, F., Sender, J., 1994, "LDA Measurements In the Near Wall Region of an Axisymmetric Sudden Expansion", *Proc. 7th Int. Symp. on Applications of Laser Techniques to Fluid Mechanics*, Lisbon, Portugal, pp 13.6.1-13.6.8,
- Schlichting, H., 1979, "Boundary layer theory", 7th ed. New York: McGraw-Hill.